

A Model-Based Range Image Segmentation Algorithm Using a Novel Robust Estimator

Hanzi Wang and David Suter, Senior Member, IEEE
Department of Electrical and Computer Systems Engineering
Monash University, Clayton Vic. 3800, Australia.

{hanzi.wang ; d.suter}@eng.monash.edu.au

Abstract:

This paper presents a novel range image segmentation algorithm based on a newly proposed robust estimator: *Adaptive Scale Sample Consensus (ASSC)* [28]. The proposed algorithm is a model-based top-down technique and directly extracts the required primitives (models) from the raw images. Compared with current popular methods (region-based and edge-based methods), the algorithm is very robust to noisy or occluded data due to the adoption of the novel robust estimator ASSC. Using a hierarchical implementation, the proposed method is computationally efficient. Experimental results on real range images show that the proposed algorithm is attractive when compared with other state-of-the-art segmentation methods.

1. Introduction

Range images provide three-dimensional geometric information, related to a known reference coordinate system, about surface points on the objects in a scene. Perception of surfaces has played a very important role in image understanding, three-dimensional object recognition, robotic grasping, autonomous navigation, medical diagnosis, etc. Segmenting range images into homogeneous regions (such as the regions having the same model parameters) is the first step to recognise 3D objects. Whether or not we can correctly segment the range images is an important factor that affects the recognition of a 3D object. There are many definitions of segmentation [1, 8]. Put simply, segmentation is to break the image into some meaningful non-overlapping homogeneous regions whose union is the entire image. The methods for range image segmentation can be roughly classified into three categories:

1. Region-based segmentation techniques or clustering techniques [7, 12, 3]
2. Edge-based segmentation techniques [4, 29].
3. Primitive-based (also called model-based) techniques [30, 22, 16, 14, 13].

The essence of region growing techniques is that they segment range images based upon the similarities of feature vectors (corresponding to pixels) in range images. The region-based techniques first estimate the feature vectors at each pixel, and then aggregate the pixels that have similar feature vectors, while at the same time, separating the pixels whose feature vectors are dissimilar. However, the positions of the initial seeds greatly affect the performance of most region-based methods. When the seeds are placed on a boundary or a noise corrupted part of the image, the results will break down.

In contrast to region-based techniques, the edge-based techniques employ edge operators to localize surface boundaries and are computationally efficient. However, the main difficulties of edge-based segmentation techniques are: when range images contain noise, the effectiveness of the methods is greatly reduced; when the edge pixels detected by the edge operator are not continuous, it will be difficult to link these discontinuous pixels.

The model-based (top-down) methods are appealing because it has been established that these methods have similarities to the human cognitive process [17, 5]. The model-based methods can directly extract the required primitives from the unprocessed raw range images. In contrast, it is difficult to directly extract specified primitives by the edge-based and region-based methods. In model-based approaches, primitive geometric features that are generally much higher level than the features that are used in region-based methods, are matched to the data. Then matches are checked for local consistency by employing some geometric constraints, e.g. distances, orientation of normals, etc. Because of the introduction of robust statistics into some model-based methods [30, 22, 16, 14], those methods are very robust to noisy or occluded data.

Whichever segmentation method we choose, an ideal method must:

- Be able to deal with the random measurement noises and quantization noise.
- Be able to analyze scenes that are not limited to those containing certain type of surfaces such as planar or curved surfaces.
- Not be affected by the viewing direction.
- Be able to handle arbitrary combinations of objects in arbitrary locations and orientations and be able to resist the influence of occlusions.

Unfortunately, no existing methods have all of these capabilities. To develop a method that satisfies all these requirements is a long-term task for the computer vision community.

In this paper, we develop a range image segmentation algorithm based on our recently proposed robust estimator – the ASSC (*Adaptive Scale Sample Consensus*) estimator [28]. Compared to traditional robust methods (such as least median squares (LMedS) [19], least trimmed squares (LTS) [20], and M-estimators [10], etc.), the ASSC estimator has many advantages: It can resist more than 80% outliers while most traditional robust methods can only resist up to 50% outliers; ASSC outperforms the recently proposed (similar) robust estimators: residual consensus (RSEC) [30], adaptive least kth squares (ALKS) [14], minimum unbiased scale estimator (MUSE) [16], etc., for data with multiple structures; ASSC does not need prior knowledge about the scale estimate of inliers; It simultaneously yields the parameters of a model and the corresponding scale.

This paper is organized as follows: in section 2, the procedure of the ASSC method is described and its achievements over other popular robust estimators are evaluated. In section 3, a robust range image segmentation algorithm is proposed and the procedure of the algorithm is illustrated. The experimental results of the proposed algorithm on real range images are presented and compared with the results of other state-of-the-art segmentation methods in section 4. Finally, we conclude in section 5.

2. Robust Fitting and Scale Estimation

An important goal of computer vision algorithms is to extract geometric information from an image. Parametric models play a vital role in computer vision research. It has been widely recognised that it is almost unavoidable that data are contaminated (due to sensor noise, faulty feature extraction, etc) and it is also likely that the data will include multiple structures. Thus, computer vision algorithms are required to be robust [6].

During the past several decades, a number of robust estimators have appeared in the literature. Roughly, we can classify these robust estimators into two categories:

- 1) Traditional estimators (such as LMedS [19], LTS [20], M-estimators [10], etc.). These estimators are characterized by the fact that their breakdown points are no more than 50%, i.e., when gross outliers occupy more than 50% of the whole data, these estimators will totally break down.

- 2) Recently proposed estimators (e.g., RANSAC [2], Hough Transform [9, 11], ALKS [14], RESC [30], MUSE [16], MINPRAN [22]). These estimators have an important property: they can tolerate the influence of more than 50% outliers.

The second category of estimators has received more and more attention in computer vision community because outliers and multiple structures (which may occupy more than 50% of the whole data) occur in many applications.

Among the second category of estimators, the Hough transform and the RANSAC method were developed within the computer vision community (as opposed to being seen as general purpose statistical procedures) and widely used in vision tasks. Both techniques can achieve good results for data with more than 50% outliers. However, they need a user to provide a priori and estimate of the scale, which is not available in most practical tasks. Moreover, the other shortcomings of the Hough Transform are excessive storage requirements and computational complexity in high dimensional parameter spaces.

RESC, MINPRAN, MUSE, ALKS, etc. all claimed that they can tolerate more than 50% outliers. However, RESC needs the user to tune many parameters in compressing histogram. MINPRAN assumes that the outliers are randomly distributed within a certain range, which makes MINPRAN less effective in extracting multiple structures. MUSE and ALKS are limited in their ability to handle extreme outliers.

The ASSC estimator is newly proposed robust estimator [28]. The estimator needs not priori knowledge about the scale of inliers. It automatically outputs the scale and the parameters of a model. Next, we will introduce this recently developed ASSC estimator.

2.1 The ASSC estimator.

We explain this method by referring to a prototypical-fitting problem: plane fitting. A plane equation can be written as:

$$Z=AX+BY+C \quad (1)$$

Where (A, B, C) are the parameters of a plane. Denote by $\{(X_i, Y_i, Z_i)\}_{i=1,..,n}$ the sample points. The parameters of a plane can be determined by p points (p=3). For the given parameters (A, B, C), the residual of the point at (X_i, Y_i, Z_i) is:

$$r_i=Z_i-AX_i-BY_i-C \quad (2)$$

Normally, the residuals of inliers are assumed to have a Normal distribution $N(0, \sigma)$.

- 1) Randomly choose a p-subset (p=2 for a line model, or 3 for planar model).
- 2) Calculate the ordered absolute residuals using the parameters determined by the p-subset, and calculate the bandwidth for TSSE.
- 3) Apply TSSE to estimate the scale of inliers.
- 4) Validate the valley. If the valley is valid, go to step 5); otherwise, go to step 1.
- 5) Calculate the objective function of ASSC (i.e., assigning each p-subset candidate a score).
- 6) Repeat step 1) to 5) m times. Finally, output the parameters and scale corresponding to the maximum score as results.

Figure1. Robust ASSC algorithm

The random sampling technique, which has been used in a lot of robust methods (LMedS, LTS, RANSAC, ALKS, etc.), is employed in ASSC. There are several methods to choose p-subsets [19, 30, 25]. Statistically, one performs m times the random selections of p-subsets, so that the probability P that at least one of the m p-subsets is “clean” (i.e., it does not include outliers) is almost 1. Let ε be the fraction of outliers contained in the whole set of points. The probability P can be expressed as follows ([20], pp.198):

$$P=1-(1-(1-\varepsilon)^p)^m \quad (3)$$

Thus one can determine m for given values of ε , p and P by:

$$m = \frac{\log(1-P)}{\log[1-(1-\varepsilon)^p]} \quad (4)$$

The ASSC estimator performs a statistical analysis of the residuals to the fit for each p-subset (see figure 1). Mathematically, the ASSC estimator can be written as:

$$\hat{\theta} = \arg \max_{\theta} (n_{\theta} / S_{\theta}) \quad (5)$$

where S_{θ} is the scale of inliers. n_{θ} is the number of data points near or on the model, which are distributed within the S_{θ} related threshold T (usually, T is set as $2.5S_{\theta}$); And $\hat{\theta}$ is the estimated parameters of a model (by a p-subset of the data satisfying some condition: in our case, the maximum score of ASSC objective function: $n_{\hat{\theta}} / S_{\hat{\theta}}$).

The second ingredient of ASSC is to use kernel estimators to characterise the probability distribution of the residuals. These kernel methods require a parameter h , called the bandwidth. A simple overs-smoothed bandwidth selector [26] can be employed.

$$\hat{h} = \left[\frac{243R(K)}{35u_2(K)^2n} \right]^{1/5} S \quad (6)$$

where $R(K) = \int_{-1}^1 K(\zeta)^2 d\zeta$ and $u_2(K) = \int_{-1}^1 \zeta^2 K(\zeta) d\zeta$. K is the Epanechnikov kernel [21] and S is the sample standard deviation. In order to avoid over-smoothing, the bandwidth can be set as $c\hat{h}$, where c is a correct factor ($0 < c < 1$) ([26], p.62).

Another vital ingredient in our procedure it to use the Two-Step Scale Estimator (TSSE):The procedure of the TSSE [28] is shown in figure 2. The TSSE is used to estimate the scale in the corresponding parametric space for each p-subset. Because the residuals of inliers are assumed to have a Gaussian-like distribution (in fact, this is not an exact requirement), the validation of the ASSC can be checked by validating the valley:

$$\lambda = \hat{f}(\text{valley}) / \hat{f}(\text{peak}) \quad (7)$$

where $\hat{f}(x)$ is the probability density at x , and $1 > \lambda \geq 0$ When the valley is valid, λ should be small (in our case, for a valid valley, $\lambda < 0.8$).

- 1) Apply the mean shift method with initial center 0 to find the local peak. And apply the mean shift valley method [28] to find the local valley next to the peak.
- 2) Estimate the scale by the median scale estimator on points within the obtained valley.

Figure 2. TSSE algorithm

Though the performance of the ASSC estimator has been illustrated in [28] (including the applications of ASSC to 2D and 3D data, experimental comparisons of the achievements of RESC, ALKS, LMedS and ASSC, and quantitative results of the four methods for the estimation of the scale of inliers), in the next subsection, we will further elaborate on the performance of the ASSC estimator. We choose the traditional LMedS estimator and the recently proposed RESC and ALKS estimators for comparison. We do not choose Hough Transform and RANSAC for

comparison because these two estimators, unlike LMedS, RESC and ALKS, require the user to set parameters that effectively relate to setting/deciding the scale a priori.

2.2. Performance evaluation of the ASSC estimator and other popular robust estimators

2.2.1. The breakdown plot of the four methods

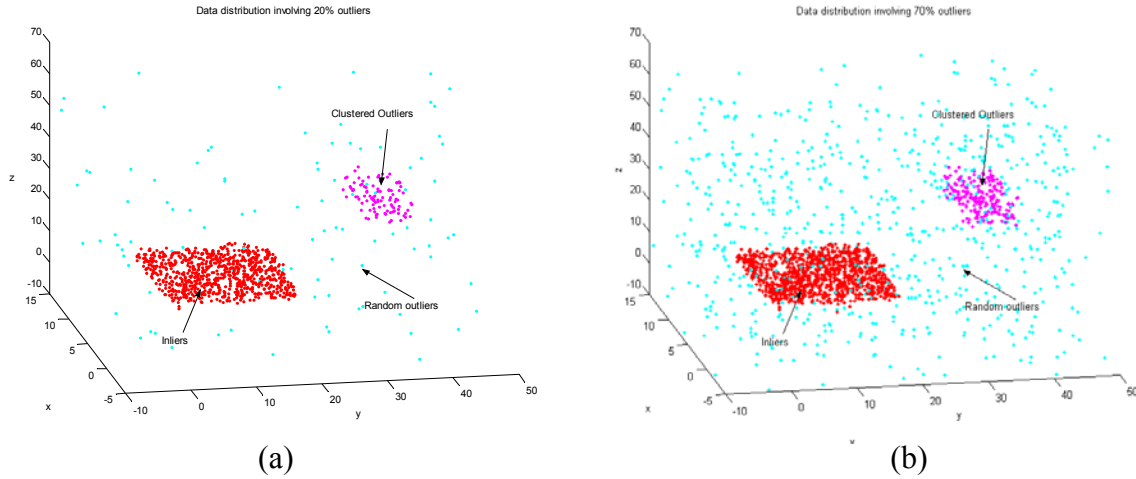


Fig. 3. Distributions of the data with (a) 20% outliers; (b) 70% outliers.

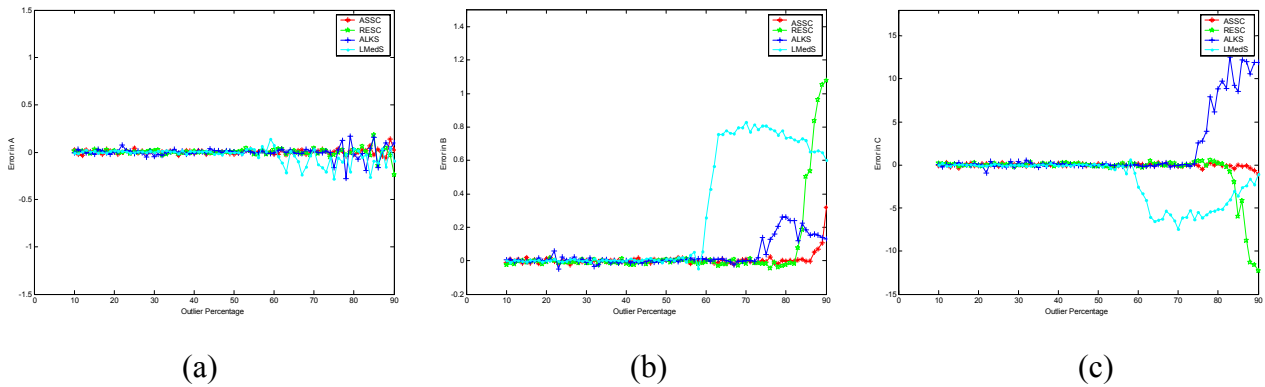


Fig. 4. Breakdown plot of the four methods

First, we perform an experiment to draw the breakdown plot of each method (similar to the experiment reported in [30]). However, the data that we use is more complicated because it contains two types of outliers: clustered outliers and randomly distributed outliers). We generate one plane signal with Gaussian noise having unit standard variance. Both clustered outliers and randomly distributed outliers are added to the data. The clustered outliers have 100 data points and

are distributed within a cube. The randomly distributed outliers contain the plane signal and clustered outliers. The number of inliers is decreased from 900 to 100. At the same time, the number of randomly distributed outliers is increased from 0 to 750 so that the total number of the data points is kept 1000. Thus, the outliers occupy from 10% to 90% outliers. Examples for data with 20% and 70% outliers are shown in figure 3 to illustrate the distributions of the inliers and outliers. If an estimator is robust enough to outliers, it can resist the influence of both clustered outliers and randomly distributed outliers even when outliers occupy more than 50% of the data. In order to increase the stability of the result, we perform the experiments 20 times, using different random sampling seeds, for each data set involving different percentage of outliers (10% to 90%). An averaged result is show in figure 3.

From figure 4, we can see that our method obtains the best achievement. Because the LMedS has only 50% breakdown point, it broke down when outliers approximately occupied more than 50% of the data. ALKS broke down when outliers had about 75%. RESC began to break down when outliers had more than 83% of the whole data; In contrast, the ASSC estimator is the most robust to outliers. It began to breakdown at 89% outliers. In fact, when inliers are about or less than 10% of the data, the assumption that inliers should occupy a relative majority of the data is violated. Bridging between the inliers and the clustered outliers tends to yield a higher score. Other robust estimators also suffer from the same problem.

2.2.2. The influence of the noise level of inliers on the results of robust fitting

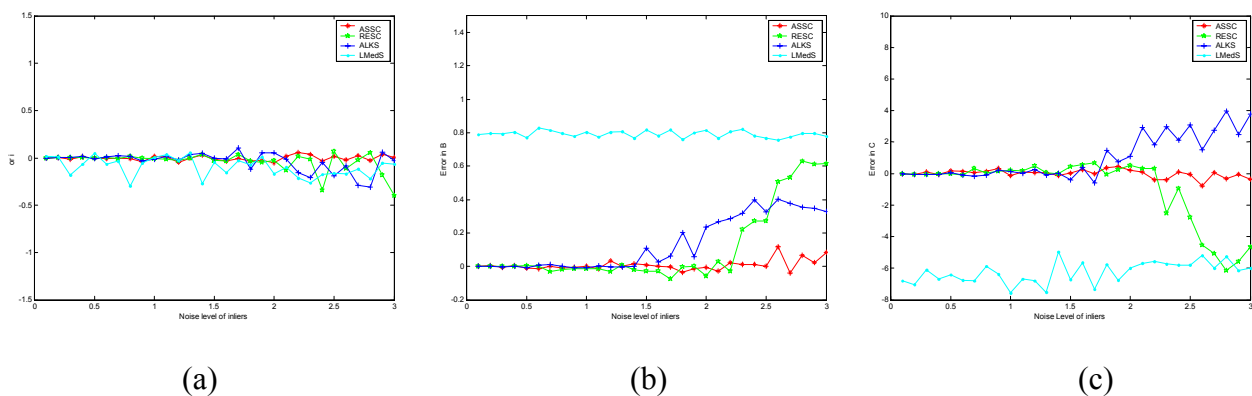


Fig. 5. The influence of the noise level of inliers on the results of the four methods

Next, we will investigate the influence of the noise level of inliers on the results of the chosen four robust fitting methods. We use the signal shown in figure 3 (b) with 70% outliers. But we change the standard variance of the plane signal from 0.1 to 3, with interval 0.1.

Figure 5 shows that LMedS broke down first. This is because that LMedS cannot resist the influence of outliers when the outliers occupy more than a half of the data points. ALKS, RESC, and ASSC estimators all can tolerate more than 50% outliers. However, among these three robust estimators, ALKS broke down first. It began to break down when the noise level of inliers is increased to 1.7. RESC is more robust than ALKS: it began to break down when the noise level of inliers is increased to 2.3. The ASSC estimator shows the best achievement. Even when the noise level is increased to 3.0, the ASSC estimator did not break down yet.

2.2.3. The influence of the relative height of discontinuous signals on the results of the four methods

Discontinuous signals (such as parallel lines/planes, step lines/planes, etc.) often appear in computer vision task. Work has been done to investigate the behavior of robust estimators for discontinuous signals [16, 23, 24]. Discontinuous signals are hard to deal with: e.g., most robust estimators break down and yield a “bridge” between the two planes of a “one step” signal. The relative height of the discontinuity is a crucial factor. In this subsection, we will investigate the influence of the discontinuity on the performance of the four comparative robust estimators.

We generate two discontinuous signals: one containing two parallel planes and one containing “one-step” planes. The signals have unit variance. Randomly distributed outliers covering the regions of the signals are added to the signals. Among the total 1000 data points, there are 20% pseudo-outliers and 50% random outliers. The relative height is increased from 1 to 20. Figure 6 (a) and (b) shows examples of the data distributions of the two signals with relative height 10. The averaged results over 20 times obtained by the four robust estimators are shown in figure 6 (c1-c3) and (d1-d3). From figure 6, it seems that there is a virtual “adherent force” between the discontinuous signals. The less the relative height is, the more the “adherent force” is; vice versa. If an estimator is robust to discontinuous signals, the estimator can tolerate the influence of the “adherent force”.

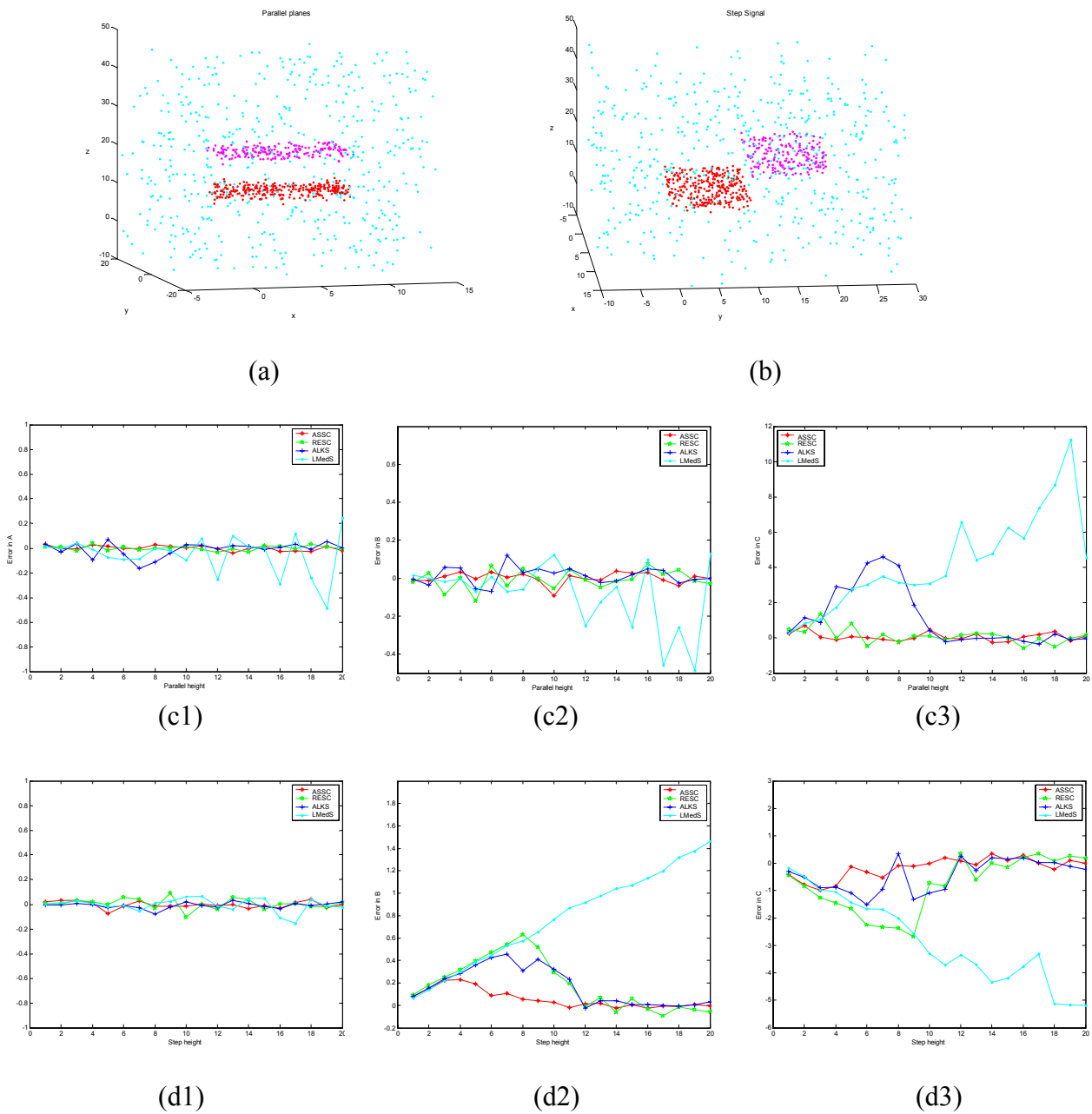


Fig. 6. The influence of the relative height of discontinuous signals on the results of the four methods: (a) two parallel planes; (b) one step signal; (c1-c3) the results for the two parallel planes; (d1-d3) the results for the step signal.

LMedS shows the worst results among the four robust estimators. It cannot tolerate the influence of the “adherent force”. This is because the data involve 70% outliers. The rest three estimators (RESC, ALKS, ASSC) can tolerate more than 50% outliers.

From figure 6 (c1-c3) and (d1-d3), we can see that:

- for the parallel plane signal, the results by ALKS are affected more by the “adherent force”: when the relative height is small, the “adherent force” tends to affect the results of ALKS heavily; when the relative height is large enough (10 or more), the “adherent force” is small. ALKS is robust to outliers again. As comparisons, RESC and ASSC estimators show better robustness to the “adherent force”.
- for the step signal, when the step height is small, the “adherent force” affects all of these three estimators. When the step height is increased from small to large, ASSC shows the robustness to the “adherent force” first. The ASSC estimator completely tolerates the influence of the “adherent force” when the step height is larger than 5. RESC and ALKS have similar results. RESC and ALKS resist the influence of the “adherent force” only when the step height is 12 or more.

In next section, we will apply the ASSC estimator to a more complicated computer vision task: range image segmentation.

3. A hierarchal Algorithm for range image segmentation

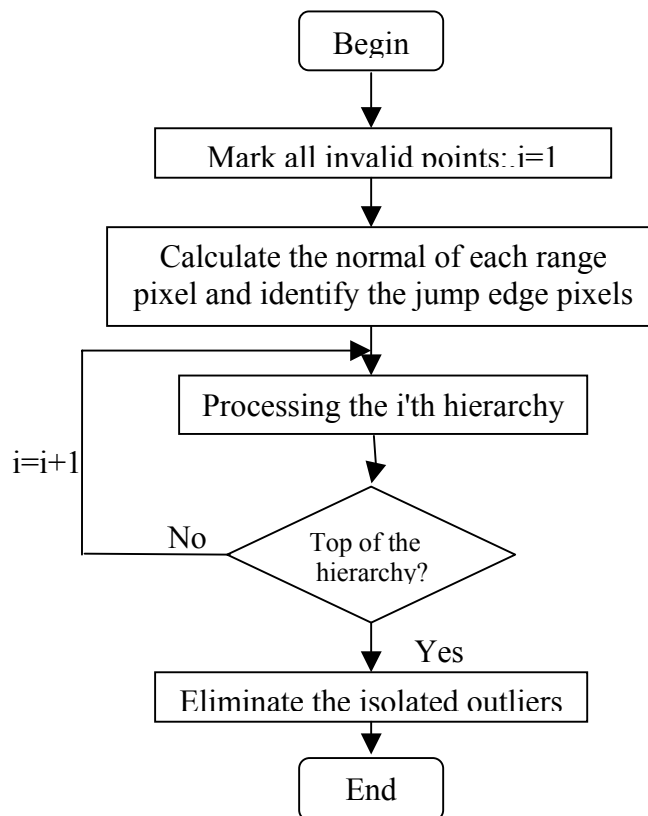


Fig. 7. Range image segmentation algorithm

Range image segmentation is a complicated task because range images may contain many gross errors (such as sensor noise, etc.) as well as containing multiple structures. Many robust estimators have been employed to segment range images (such as [18, 30, 22, 16, 14, 13], etc.). For a simple range image, it is possible that one structure occupies the absolute majority of the whole data. However, in general, any single structure in a range image usually cannot occupy an absolute majority of the whole data. In these cases, an algorithm employing traditional robust estimators such as LMedS, whose breakdown point is no more than 50%, has to split the range image into several small patches and segment each patch, and finally, merge the results of each small patch according to some homogeneity criterion. Moreover, if no structure in a small patch is more than 50% of the data in the patch, the result will break down.

However, even if an algorithm employs a more highly robust estimators, such as RESC, ALKS, etc., the robust estimator cannot be directly applied to segment range images effectively. Several practical issues must also be considered:

1. The computational cost. Range image usually involves a large number of data points (often hundreds of thousands of data points). Thus, the computational complexity of robust estimators must be considered.
2. Handling of intersections of surfaces. When two surfaces intersect, points around the intersection line may possibly be assigned to either surface. In fact, the intersection line is on the both surfaces and the data points are inliers to the both surfaces. Additional information (such as the normal to the surface at each pixel) should be used to handle data near the intersection line.
3. Handling virtual intersection. The data points of each segmented surface should be connected. However, it happens that two surfaces do not actually intersect, but the extension of one surface is intersected by the other surface. In this case, the connected component algorithm [15] should be employed.
4. Removal of the isolated outliers. When all surfaces are estimated, some isolated outliers, due to the noise introduced by range image camera, may remain. At this stage, a post processing procedure should be made to eliminate the isolated outliers.

The originators of other novel estimators (e.g. ALKS, RESC, MUSE, MINPRAN) have applied their estimators to range image segmentation, but they have not generally tackled all of the above

issues. Hence, even those interested in applying ALKS/RESC or any other estimator to range image segmentation may find several of the components of our complete implementation independently useful.

Our range image segmentation algorithm is shown in figure 7. We employ a hierarchy structure to make the algorithm computationally efficient. We apply our algorithm to the real range images from the USF database¹. The ABW range images were generated by using an ABW structured light scanner. Shadow pixels may occur in an ABW range image. These points cannot give range information and thus will not be processed. All ABW range images have 512x512 pixels. There are four level hierarchies in total used in our algorithm. The bottom level of the hierarchy contains 64x64 pixels that are obtained by using regularly sampling on the original image. The top level of the hierarchy is the original image. The second level and the third level of the hierarchy have 128x128 and 256x256 pixels respectively. We begin with bottom of the hierarchy, i.e., the 64x64 regular sampled range image, and proceed back up to higher level of the hierarchy, until the top hierarchy, i.e., 512x512 range image.

For unlabelled points in the top hierarchy, we use the connected component algorithm to get the maximum connected component. Thus, the data for current hierarchical level can be obtained by regularly sampling on the maximum connected component. For the connected points whose number is below a threshold, we marked them as noise.

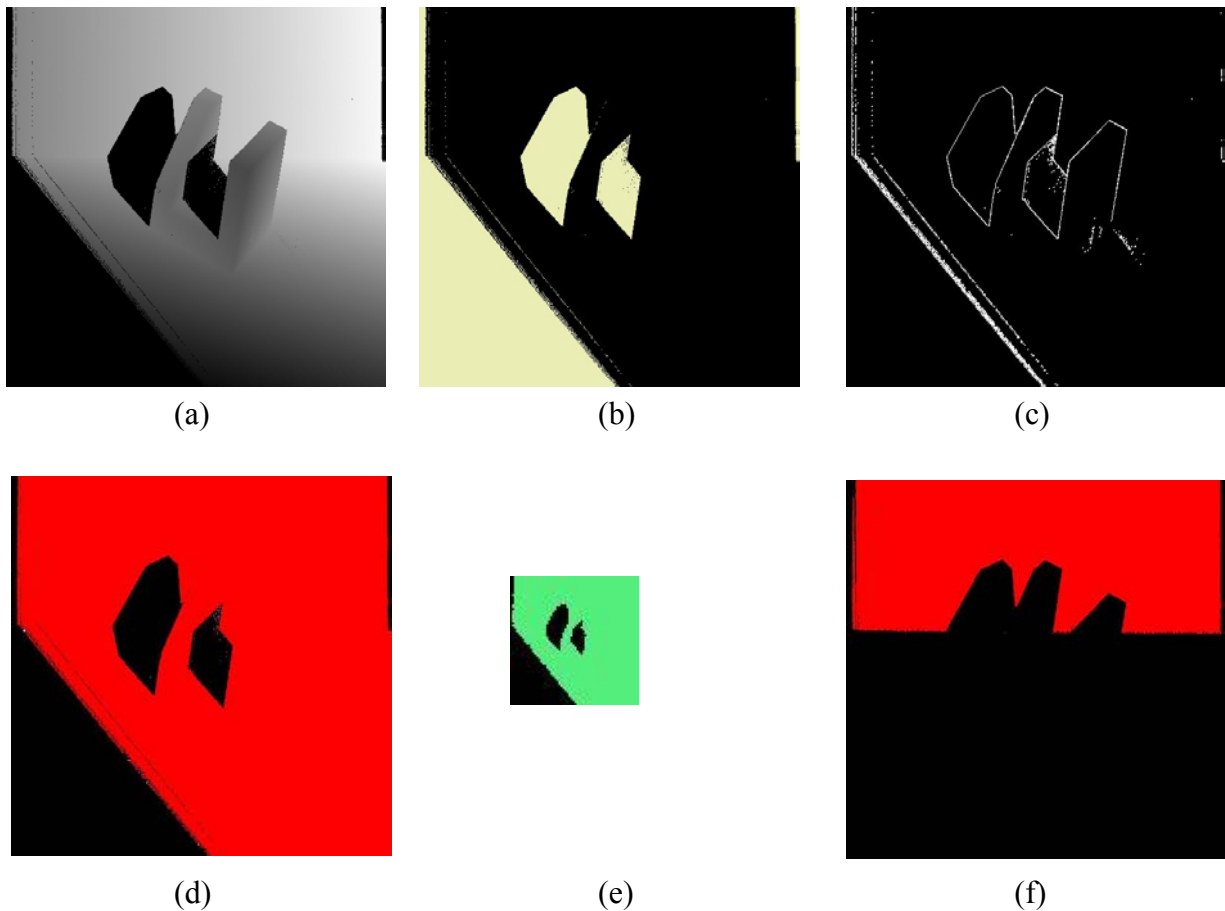
In each level of the hierarchy, we:

- (1) Apply the ASSC estimator to obtain the parameters of plane and the scale of inliers.
- (2) The inliers (in the top of the hierarchy) corresponding to the estimated parameters of plane and scale are then identified. If the number of inliers is less than a threshold, go to step (7).
- (3) Using normal information to validate the inliers obtained in step (2). The normal of inliers should be homogenous. When the angle between the normal of the data point that has been classified as an inlier, and the normal of the estimated plane, is less than a threshold value, the data point is accepted. Otherwise, the data point is rejected and will be used as some of the left-over points for further processing. If the number of the validated inliers is small, go to step (7).
- (4) Filling in the holes inside the maximum connected component from the validated inliers. The holes may appear because the sensor noises or some points have large residuals and beyond the range that the estimated scale can cover.

¹ <http://marathon.csee.usf.edu/seg-comp/SegComp.html>

- (5) Assign label to the points corresponding to the connected component from step (4) and remove the points from the data set that will be further processed. This happens in the top hierarchy.
- (6) If a point is unlabelled and it is not a jump edge point, the point will be used as a left-over point. After collecting all left points, using the connected component algorithm to get the maximum connected component. If the number of the maximum connected component is smaller than a threshold, go to step (7); otherwise, get the data for the current hierarchical level by regularly sampling on the maximum connected component obtained in step 6, then go to step (1).
- (7) Terminate the processing in the current level of the hierarchy and go to the higher-level hierarchy until the top of the hierarchy.

Part of the procedures of the proposed algorithm is illustrated in figure 8.



(continued over page)

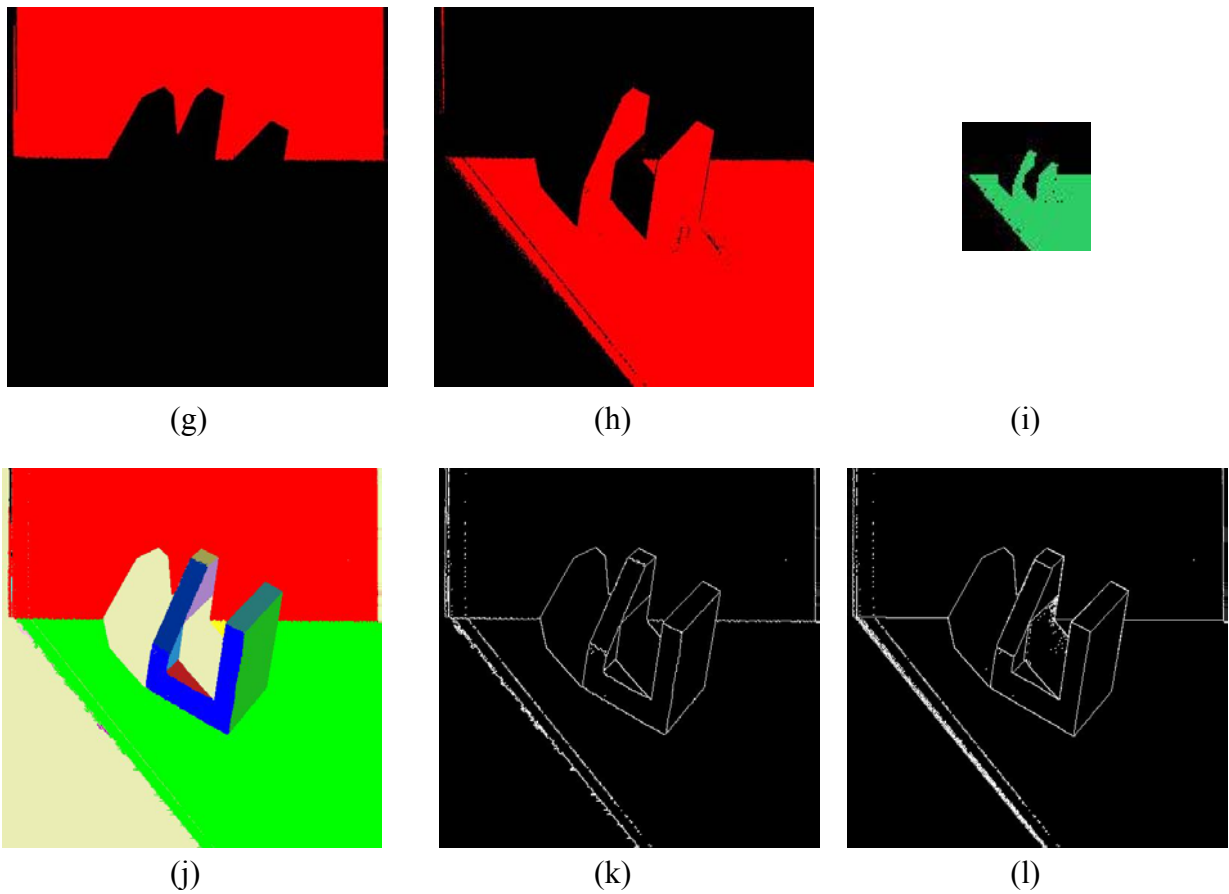


Fig. 8. Range image segmentation by the proposed method. (a) Range image (ABW test.22 from the USF database); (b) The marked invalidated points; (c) the detected jump edge points; (d) the first connected component to be processed; (e) the bottom of the hierarchy (i.e., the first-level hierarchy: that is a 64x64 regularly sampled image); (f) the first detected plane with holes using the parameters obtained by the ASSC estimator; (g) The result after filling holes; (h) the points left-over after removing the first plane; (i) the points with maximum connected component for further processing in the same level of hierarchy; (j) the final result; (k) The edge image of the segmented result; (l) the ground truth result.

4. Experiments

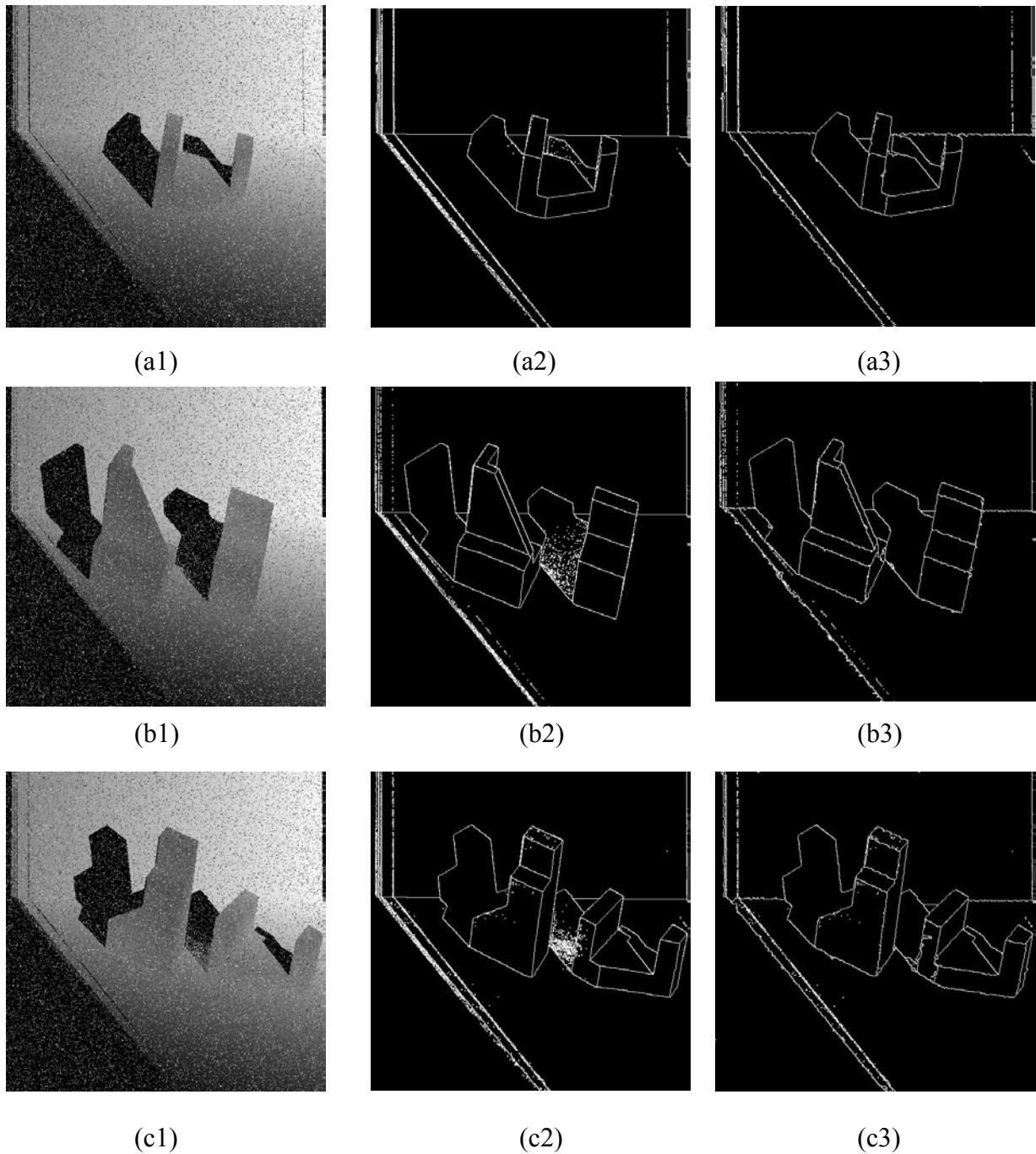


Fig. 9. Segmentation of ABW range images from the USF database. (a1, b1, c1) Range image with 26214 random noise points; (a2, b2, c2) The ground truth results for the corresponding range images without adding random noise; (a3, b3, c3) Segmentation result by the proposed algorithm.

Due to the adoption of the robust ASSC estimator, the proposed range image segmentation is very robust to noise. In order to show the advantages of the proposed method, we added 26214 random noise points to the range images taken from the USF ABW range image database (test 16, test7 and train 5). At the beginning of the segmentation, there are a high percentage of random outliers

(from random noise) and pseudo outliers (from multiple structures) contained in the data. No noise filter method is performed. We directly segment the unprocessed raw images.

As shown in figure 9, all of the main surfaces were recovered by our method. Only a slight distortion appeared on some boundaries of neighboring surfaces. This is because of the sensor noise and the limited accuracy of the estimated normal at each range point. In fact, the more accurate the range data are, and the more accurate the estimated normals at range points are, the less the distortion is.

We also compare our results with those of several state-of-the-art approaches [8] of the University of South Florida (USF), Washington State University (WSU), and the University of Edinburgh (UE). Figure 10 (c-f) and figure 11 (c-f) show the results obtained by the four methods. All of the segmented results by the four methods should be compared with the results of the ground truth (figure 10 (b) and figure 11 (b)).

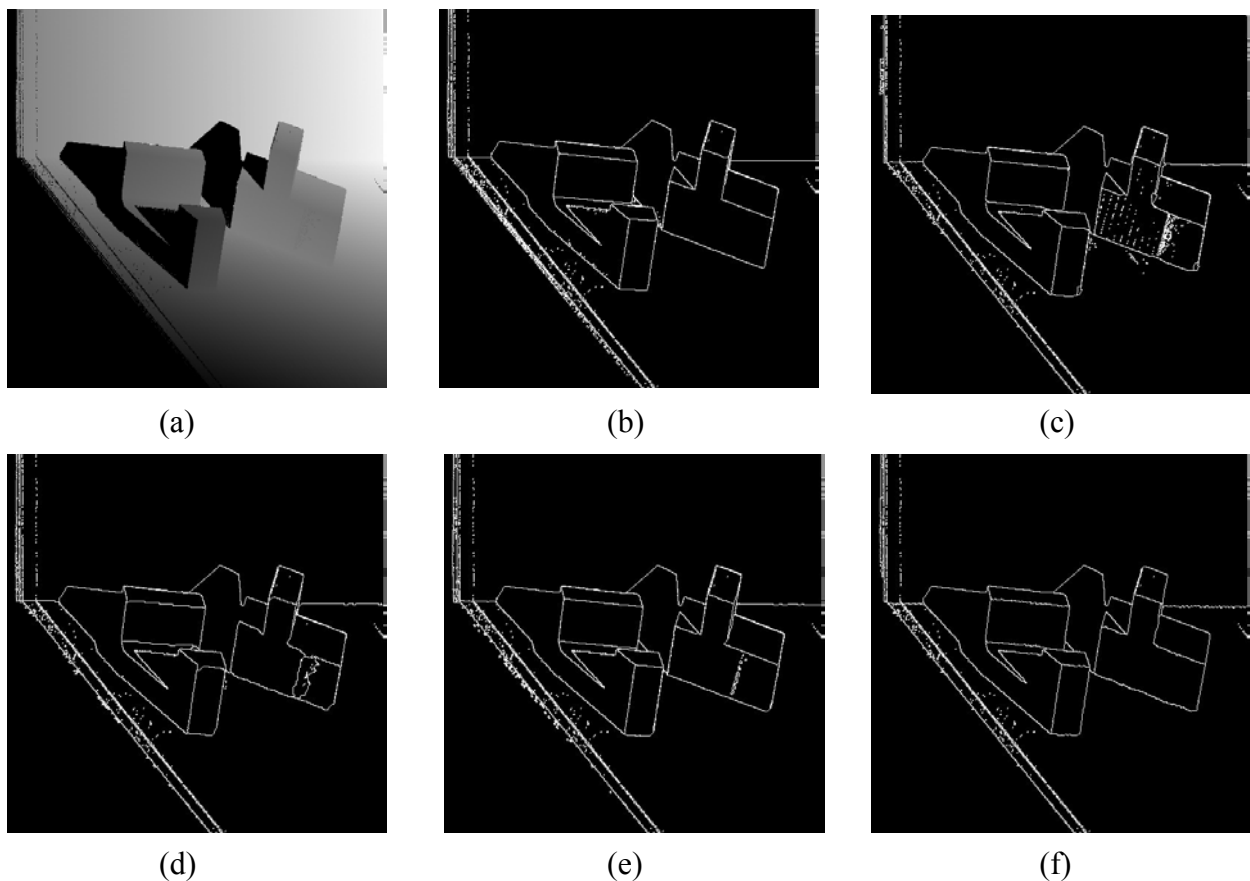


Fig.10. Comparison of the segmentation results for ABW range image (test 3) from the USF range image database. (a) Range image; (b) The result of ground truth; (c) The result by the USF;(d) The result by the WSU; (e) The result by the UE; (f) The result by the proposed method.

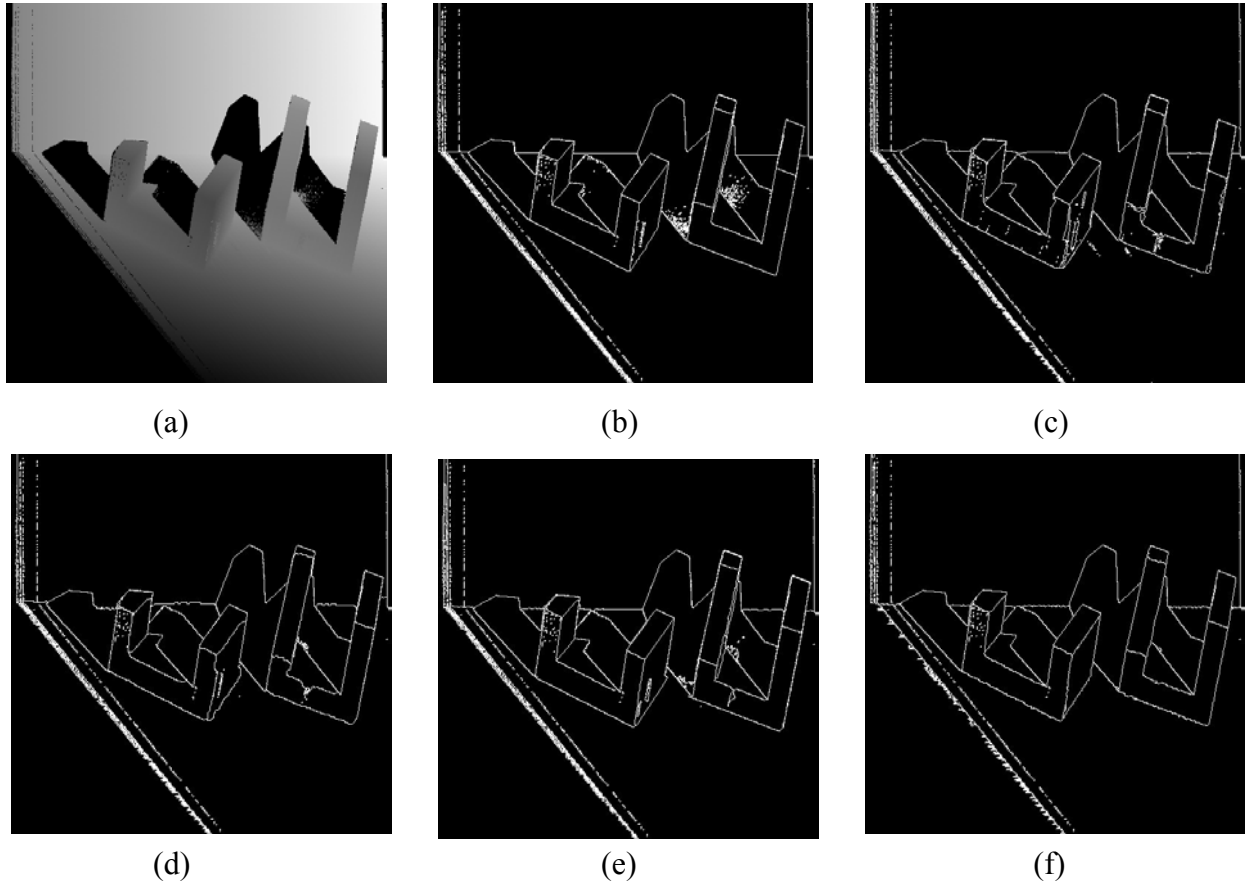


Fig. 11. Comparison of the segmentation results for ABW range image (test 13) from the USF range image database. (a) Range image; (b) The result of ground truth; (c) The result by the USF; (d) The result by the WSU; (e) The result by the UE; (f) The result by the proposed method.

From figure 10 (c) and figure 11 (c), we can see that the USF's results contained many noisy points. In both figure 10 (d) and figure 11 (d), the WSU segmenter missed one surface. The WSU segmenter also over segmented one surface in figure 10 (d). Some boundaries on the junction of the segmented patch by the USF and WSU in figure 11 (c) were relatively seriously distorted. The UE shows relatively better results than those of USF and the WSU. However, some estimated surfaces are still noisy (see figure 10 (e) and figure 11 (e)). Compared with the other three methods, the proposed method achieved the best results. All surfaces are recovered and the segmented surfaces are relatively "clean". The edges of the segmented patches were reasonably good.

Our method directly extracts the planar primitives from the raw range data. Adopting hierarchy-sampling technique in the proposed method greatly reduces its time cost. The processing time of the method is affected to a relatively large extent by the number of surfaces in the range images. The processing time for a range image including simple objects is faster than that for a range

image including complicated objects. Generally speaking, given $m=500$, it takes less than one minute (on an AMD800MHz personal computer in C interfaced with MATLAB language) for segmenting a range image with simple surfaces and about 1-2 minutes for a range image including complicated surfaces. This includes the time for computing normal information at each range pixel (which takes about 12 seconds).

5. Conclusion

The ASSC estimator is a newly proposed promising estimator and it can tolerate more than 50% outliers. In this paper, we explore the properties of the ASSC estimator for 3D data and discontinuous signals. The results of the ASSC estimator are also compared to several popular robust estimators: LMedS, RESC, and ALKS. Experiments show that the ASSC estimator achieves better results than the other three estimators, and provides a better alternative choice in computer vision tasks where the estimator should be robust to data with a high percentage of outliers and multiple structures.

Based on the ASSC estimator, we propose a model-based top-down algorithm for range image segmentation. The advantages of employing the ASSC estimator in our algorithm are that the ASSC estimator needs not a priori knowledge about the scale of inliers: it yields both the parameters of a geometric primitive, and the corresponding scale of the noise. Moreover, it has high robustness to outliers and multiple structures, and it provides good performance in fitting discontinuous signal. This makes the ASSC estimator highly efficient in the range image segmentation task. In [27], we have successfully applied our previously proposed QMDP estimator to robust optical flow calculation. In our future work, we will explore the application of this newly proposed ASSC estimator to the field of robust optical flow calculation.

References

1. Ballard, D.H. and C.M. Brown, *Computer vision*, ed. N.J.P. Hall. 1982.
2. Fischler, M.A. and R.C. Rolles, *Random Sample Consensus: A Paradigm for Model Fitting with Applications to Image Analysis and Automated Cartography*. Commun. ACM, 1981. **24**(6): p. 381-395.
3. Fitzgibbon, A.W., D.W. Eggert, and R.B. Fisher, *High-Level CAD Model Acquisition from Range Images*. Technical Report, Dept. of Artificial Intelligence, Univ. of Edinburgh., 1995.
4. Ghosal, S. and R. Mehrotra, *Detection of Composite Edges*. IEEE Trans. PA, 1994. **13**(1): p. 14-25.

5. Gregory, R.L., *The intelligent Eye*. New York:McGraw-Hill., 1970.
6. Haralick, R.M., *Computer vision theory: The lack thereof*. Comput. Vision Graphics Image Processing, 1986. **36**: p. 372-386.
7. Hoffman, R.L. and A.K. Jain, *Segmentation and Classification of Range Images*. IEEE Trans. Pattern Analysis and Machine Intelligence, 1987. **9**(5): p. 608-620.
8. Hoover, A., G. Jean-Baptiste, and X. Jiang., *An Experimental Comparison of Range Image Segmentation Algorithms*. IEEE Trans. Pattern Analysis and Machine Intelligence, 1996. **18**(7): p. 673-689.
9. Hough, P.V.C., *Methods and means for recognising complex patterns*, in *U.S. Patent 3 069 654*. 1962.
10. Huber, P.J., *Robust Statistics*. New York, Wiley, 1981.
11. Illingworth, J. and J. Kittler, *A survey of the Hough transform*. Computer Vision, Graphics, and Image Processing, 1988. **44**: p. 87-116.
12. Jiang, X.Y. and H. Bunke, *Fast Segmentation of Range Images into Planar Regions by Scan Line Grouping*. Machine Vision and Applications, 1994. **7**(2): p. 115-122.
13. Koster, K. and M. Spann, *MIR: An Approach to Robust Clustering--Application to Range Image Segmentation*. IEEE Trans. Pattern Analysis and Machine Intelligence, 2000. **22**(5): p. 430-444.
14. Lee, K.-M., P. Meer, and R.-H. Park, *Robust Adaptive Segmentation of Range Images*. IEEE Trans. Pattern Analysis and Machine Intelligence, 1998. **20**(2): p. 200-205.
15. Lumia, R., L. Shapiro, and O. Zungia, *A New Connected Components Algorithm for Virtual Memory Computer*. Computer Vision, Graphics, and Image Processing, 1983. **22**(2): p. 287-300.
16. Miller, J.V. and C.V. Stewart. *MUSE: Robust Surface Fitting Using Unbiased Scale Estimates*. in *Proc. Computer Vision and Pattern Recognition, San Francisco*. 1996: p. 300-306.
17. Neisser, U., *Cognitive Psychology*. New York: Appleton-Century-Crofts, 1967.
18. Roth, G. and M.D. Levine, *Segmentation of Geometric Signals using Robust Fitting*. Proc. 10th. Conf. on Pattern Recognition, 1990. **1**: p. 826-831.
19. Rousseeuw, P.J., *Least Median of Squares Regression*. J. Amer. Stat. Assoc, 1984. **79**: p. 871-880.
20. Rousseeuw, P.J. and A. Leroy, *Robust Regression and outlier detection*. John Wiley & Sons, New York., 1987.
21. Silverman, B.W., *Density Estimation for Statistics and Data Analysis*. 1986, London: Chapman and Hall.
22. Stewart, C.V., *MINPRAN: A New Robust Estimator for Computer Vision*. IEEE Trans. Pattern Analysis and Machine Intelligence, 1995. **17**(10): p. 925-938.

23. Stewart, C.V., *Bias in Robust Estimation Caused by Discontinuities and Multiple Structures*. IEEE Trans. Pattern Analysis and Machine Intelligence, 1997. **19**(8): p. 818-833.
24. Stewart, C.V., *Robust Parameter Estimation in Computer Vision*. SIAM Review, 1999. **41**(3): p. 513-537.
25. Tordoff, B. and D.W. Murray, *Guided Sampling and Consensus for Motion Estimation*. 7th European Conference on Computer Vision, 2002. **Vol.I**: p. 82-96.
26. Wand, M.P. and M. Jones, *Kernel Smoothing*. Chapman & Hall, 1995.
27. Wang, H. and D. Suter. *Variable bandwidth QMDPE and its application in robust optic flow estimation*. in *Proceedings ICCV03, International Conference on Computer Vision*. 2003. Nice, France: p. to appear.
28. Wang, H. and D. Suter. *ASSC A New Robust Estimator for Data with Multiple Structures*. in *Technical Report (MECSE-2003-8), Monash University*. 2003.
29. Wani, M.A. and B.G. Batchelor, *Edge Region Based Segmentation of Range images*. IEEE Trans. Pattern Analysis and Machine Intelligence, 1994. **16**(3): p. 314-319.
30. Yu, X., T.D. Bui, and A. Krzyzak, *Robust Estimation for Range Image Segmentation and Reconstruction*. IEEE Trans. Pattern Analysis and Machine Intelligence, 1994. **16**(5): p. 530-538.